PCCP

ARTICLE

Internal conversion outcompetes autodetachment from resonances in the deprotonated tetracene anion continuum

Received 00th January 2015,
Accepted 00th January 2015

DOI: 10.1039/x0xx00000x

www.rsc.org/

James N. Bull[a], Christopher W. West[a] and Jan R. R. Verlet[a]†

Photoelectron velocity-map imaging and electronic structure calculations have been used to study the temporary anion (resonance) dynamics of the closed-shell site-specific deprotonated tetracene anion ($C_{18}H_{11}^-$) in the $h\nu$ = 3.26 eV (380 nm) to 4.13 eV (300 nm) range. In accord with a recent frequency-, angle-, and time-resolved photoelectron imaging study on a related but open-shell polyaromatic radical anion (*Chem. Sci.*, 2015, **6**, 1578-1589), population of π*-resonances situated in the detachment continuum efficiently recover the ground electronic state of the anion through ultrafast non-adiabatic dynamics, followed by characteristic statistical electron loss (thermionic emission). The combined electron yield of direct photodetachment and autodetachment from the optically-accessed resonances in $C_{18}H_{11}^-$ is several orders of magnitude smaller than thermionic emission from the ground electronic electronic state in the photon energy range studied. This result implies a resiliance to prompt photoejection from UV radiation, and the ability of neutral PAH-like species to capture a free electron and form a long-lived molecular anion that ultimately decays by thermionic emission on a millisecond timescale. The attachment mechanism applies to polyaromatic species that cannot support dipole-bound states, and may provide an additional route to forming anions in astrochemical environments.

Introduction

Polyaromatic hydrocarbon (PAH) molecules are found across a diverse range of chemical environments. For example, they form as products in combustion and anthropogenic pollution,[1] they are used in new generation semiconductors and microelectronics,[2,3] and they have been postulated to be present in astrochemical environments.[4,5] In astrochemistry, anions are recognised as important chemical species,[6-11] and have been identified as small polyynes such as C_4H^- and C_6H^-,[12-18] and are commonly postulated to be present as PAHs. However, the detailed formation mechanism of astrochemical anions is unclear. It is commonly postulated that stable anions may be formed via electric dipole-bound doorway states;[19,20] however, most neutral PAH molecules do not have a sufficient dipole moment to support such a mechanism.

Most molecules, particularly those with π-conjugated systems, exhibit temporary anions or resonances.[21-23] Briefly, resonances are quasi-bound electronic states of the anion that are energetically situated above the neutral ground state (situated in the detachment continuum) and are formally unbound to electron ejection. In PAHs, π* orbitals are particularly efficient at capturing a free electron and, similar to dipole-capture, the dynamics of the temporary anion state determines the fate of the anion.[22] Although spontaneous autodetachment from a resonance is typically very fast (tens to hundreds of femtoseconds), non-adiabatic internal conversion can compete and even dominate.[24-28] Indeed, many electron impact studies on conjugated molecules have observed efficient formation of long-lived anions despite the incident electron energies and molecular configurations incompatible with an electric dipole-mediated capture mechanism.[22,29] As a specific example, mass spectrometry measurements on tetracene and pentacene have shown the formation of long-lived anions with lifetimes of ~10 ms following capture of electrons with up to ~3 eV of kinetic energy.[30] Internal conversion of an anion resonance converts electronic energy into vibrational excitation, which then becomes redistributed amongst the internal degrees of freedom (intramolecular vibrational relaxation) and leads to a temperature increase of the molecular anion.[31,32] If such an anion is formed under isolated conditions, the total internal energy of the system remains above the neutral ground state and the system may statistically detach the most weakly bound electron on a microsecond to millisecond timescale – known as thermionic emission.[33-37] Alternatively, some internally-hot anions may liberate excess internal energy through photoemission processes or by unimolecular dissociation to yield a stable anion.

Using pump-probe femtosecond spectroscopy we have recently shown that a conjugated quinone, menadione,[26] can very efficiently produce ground electronic state anions following photoexcitation (or electron capture) with energies up to 3 eV above-threshold and probably higher. In menadione, the

[a] *Department of Chemistry, Durham University, South Road, DH1 3LE, Durham, United Kingdom.*
† Email: j.r.r.verlet@durham.ac.uk

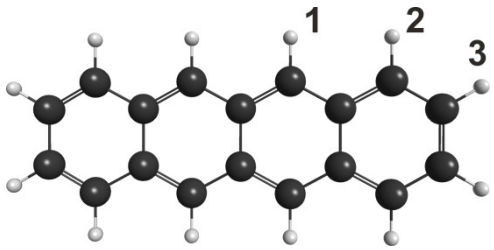

Fig. 1: Illustration of tetracene or benz[b]anthracene. Labels 1, 2, and 3 denote the three available deprotonation sites to produce the $C_{18}H_{11}^-$ species. Position 1 is the predominant deprotonation site in the present experiments. Key: charcoal – carbon; white – hydrogen.

dipole moment of the neutral (~0.7 D) is well below the threshold for any dipole-bound mechanism (>2.5 D),[20] which is commonly invoked for PAH or highly conjugated molecular anion formation in astrochemistry. Efficient electron capture yielding long-lived anions has been experimentally observed across a range of similar quinone molecules.[38] For menadione, recovery of the ground electronic state anion is achieved through a series of ultrafast internal conversion events between a manifold of electronic states that outcompetes prompt electron loss. We suggested that menadione may behave similarly to PAH molecules due to a similar π-delocalized valance electronic structure.

In this paper we report ultra-high vacuum photoelectron (PE) spectroscopy experiments combined with electronic structure calculations on site-specific deprotonated tetracene ($C_{18}H_{11}^-$, Fig. 1) to demonstrate the existence of similar ultrafast non-adiabatic dynamics those in menadione.[26] Our choice of the deprotonated (closed-shell) anion, $C_{18}H_{11}^-$, over the radical anion, $C_{18}H_{12}^-$, is partly for experimental reasons and because the electron affinity is larger while maintaining a similar π-system. Further, menadione illustrated the efficient non-adiabatic dynamics in an open-shell anion;[26] herein we do so for a closed-shell anion. Finally, from an astrophysical perspective, the interstellar anions that have been definitively identified are all closed-shell,[6-11,17] and astrochemical reaction rate modelling of deprotonated PAH anions has specifically supported their potential importance.[39]

In our experiment, rather than directly attaching an electron, we start with a stable anion and photoexcite some of the same resonances that are accessed by electron capture. Provided the geometries of the anion and neutral are reasonably similar, the non-adiabatic dynamics and energetics are comparable. This caveat is true for the current system, where the deprotonated tetracene anion and neutral have small relative geometric changes, although the differences in photoexcitation and electron capture cross-sections cannot be probed in these experiments. The advantage of the anion photoexcitation method is that PE spectra contain signatures of any non-adiabatic dynamics, which are more difficult to observe in conventional electron attachment. For $C_{18}H_{11}^-$ we show that photoexcitation up to at least 1.5 eV above-threshold is almost exclusively converted back to the ground electronic state of the anion. Further, photodetachment of the anion is shown to be very inefficient compared with photoexcitation and ground electronic state anion recovery, implying a resilience to direct UV-induced electron loss.

Experimental

The experimental set-up has been detailed in a number of recent studies.[26,27,40,41] Briefly, a ~1 mM solution of >99% purity tetracene (Sigma-Aldrich) dissolved in analytical grade toluene was electrosprayed at –5.0 kV under atmospheric conditions. Resulting gaseous ions were transferred *via* a vacuum transfer capillary into a radio frequency ring-electrode ion trap. The trapped ions were unloaded into a co-linear time-of-flight mass-spectrometer. Ions were directed to the centre of a continuous-mode penetrating field velocity-mapping assembly,[41,42] and laser pulses were timed to interact with the mass-selected ion. Ejected electrons were velocity-mapped onto a dual chevron multichannel plate (MCP) detector followed by a P43 phosphor screen and monitored by a CCD camera. The electron kinetic energy (*eKE*) scale was calibrated using the PE spectrum of I^-, and the velocity-mapping resolution is around 5%. All velocity-map image reconstructions used a polar onion peeling algorithm that allows the PE spectrum and electron ejection angular distributions to be determined.[43,44]

The laser pulses of ~6 ns duration were generated by a Nd:YAG (Continuum Surelite II-10) pumped optical parametric oscillator (Continuum Horizon I). The laser was unfocused in the interaction region and operated under reasonably low power conditions (~5 mJ per pulse) to minimise any two-photon or multiple-photon contributions. Velocity-map images were collected at various photon energies (*hν*) between 3.26 eV (380 nm) and 4.13 eV (300 nm). Each image accumulated sufficient counts to achieve a reasonable and comparable signal-to-noise ratio. All images were accumulated with a 500 ns gate on the MCP, allowing detection of any photoelectrons ejected over this timescale. Because thermionic emission in deprotonated tetracene anions will operate on a timescale of milliseconds,[30,34-37] our experiments only measure a small fraction of the true electron yield. The MCP detector gate timing was systematically varied in order to separate thermionic emission features from prompt detachment, as will be further detailed below.

Theoretical

Density functional theory (DFT) calculations were performed using the Gaussian 09 package,[45] and multi-reference perturbation theory calculations using the GAMESS-US package.[46] Initial DFT calculations used the ωB97XD//6-311++G(2df,2pd)+C*p* level of theory due to suitable performance for anion species,[47-50] and agreement with established values for tetracene.[51] The '+C*p*' in the basis set definition indicates the addition of an extra set of *p* functions with orbital exponent 0.01 to each carbon atom. All relevant zero-point energy corrections and vibrational frequencies where computed in the harmonic approximation. Franck-Condon simulations of direct photodetachment to the ground neutral (X^2A') and excited neutral ($1^2A''$) states were performed with

the 6-311++G(2df,2pd)+C*p* and 6-31+G(d,p) basis sets, respectively.[48,52] Several CCSD(T) calculations were performed to ensure the DFT methodology produces reasonable electron affinity parameters.[53]

Anion resonances were initially characterised within the TD-DFT framework.[54] Computed excited states were confirmed to represent resonances rather than discretised continuum states through a series of calculations in which the '+C*p*' orbital exponent was multiplied by a factor ranging 0.5 to 2.0.[55] A smaller orbital exponent corresponds to a more diffuse basis function. Actual resonances are the excited states that are relatively unchanged in energy with increasing diffuseness, while discretised continuum states progressively become lower in energy and the corresponding molecular orbital increasingly diffuse with increasing +C*p* diffuseness.

The TD-DFT calculations indicated the relevant molecular orbitals to include in the active space for the higher-level calculations employing the second-order XMCQDPT (extended multiconfigurational quasi-degenerate perturbation theory) framework.[56] Briefly, the reference active space considered the three highest energy π orbitals, the *p* lone pair, and all π^* orbitals. That is, a (8,13) complete active space. Calculations were performed with the 6-31+G(d,p) basis set. First, the geometry was re-optimised using the CASSCF wavefunction, and followed by computation of the anion resonances with multistate XMCQDPT theory assuming C_S point symmetry. Our earlier combined experimental and computational studies on π* resonances of *para*-quinones support that XMCQDPT with a sufficiently large reference active space and sufficiently compact basis provides a reasonable account of resonance vertical photoexcitation energies.[26,27,57]

Results and Discussion

Photoelectron spectra

Fig. 2 summarises all PE spectra as a waterfall plot. All spectra are dominated by a narrow Boltzmann-like distribution peaking at *eKE* ~ 0.05 eV. For $h\nu > 3.5$ eV, an additional broad shoulder on the high-*eKE* shoulder of the Boltzmann-like distribution can be identified. The maximum *eKE* of this feature increases commensurate with $h\nu$.

Because direct photodetachment is forbidden at very low-*eKE* by the Wigner threshold law,[58,59] the low-*eKE* feature must result from an indirect process. Experimentally, delaying the MCP gate by 50 ns relative to the laser yields only the low-*eKE* feature. This observation, together with the Boltzmann-like distribution and isotropic angular distribution (see image inset in Fig. 2), identifies the low-*eKE* feature to result from thermionic emission. The high-*eKE* shoulder (with *eKE* increasing commensurate with $h\nu$) arises from 'prompt detachment', containing contributions from both direct photodetachment and fast autodetachment. For direct photodetachment, a photon instantaneously induces electron ejection, projecting the ground state anion wavefunction onto

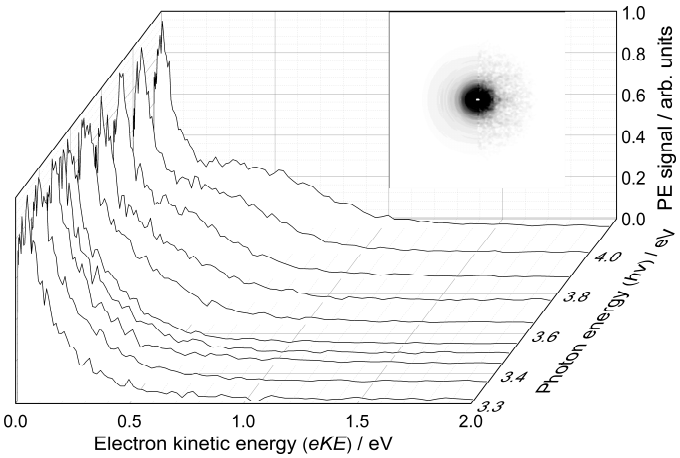

Fig. 2: All $C_{18}H_{11}^-$ photoelectron spectra as a function of photon energy ($h\nu$). Shown in the inset is the experimental central slice of the $h\nu$ = 4.13 eV (300 nm) velocity-map image (right semicircle) and reconstruction (left semicircle).

the neutral with the excess energy taken away as kinetic energy of the outgoing photoelectron. For fast autodetachment, a resonance is first photoexcited followed by spontaneous autodetachment before any non-adiabatic dynamics can occur.

The experimental prompt detachment spectrum was recovered by recording a velocity-map image in which the MCP gate was timed to record any direct or fast electron ejection plus any thermionic emission within a 500 ns window, and then subtracting an image in which the MCP gate was delayed by ~50 ns. The resulting 'prompt detachment' spectrum is shown in Fig. 3. Fig. 3 has two contributions: a weak high-*eKE* peak ($1.0 \geq eKE \geq 1.5$ eV); and an intense peak at lower *eKE* ($0 \geq eKE \geq 1.0$ eV). The high-*eKE* peak corresponds to the direct photodetachment from the ground electronic state anion to the ground electronic state neutral. Analysing all PE spectra together allows determination of the experimental adiabatic electron affinity, AEA, at 2.6 ± 0.2 eV, and the vertical detachment energy, VDE, at = 2.8 ± 0.2 eV. The peak at lower *eKE* will be assigned in the next section.

Anion resonances and energetics

Table 1 summarises calculated AEA and VDE for each of the three possible deprotonation sites shown in Fig. 1. From Table 1, deprotonation at site 1 is the only site consistent with our experimental determination of the AEA and VDE. Further, deprotonation at sites 2 and 3 are 0.20 eV and 0.26 eV than deprotonation at site 1. CCSD(T)/6-31+G(d,p) calculations at the ωB97XD geometry confirms that the functional yields reasonable AEA and VDE energetics, and also that the difference between the AEA and VDE is small and not consistent with the large low-*eKE* prompt detachment feature. Overall, the results support that only one isomer is present under our experimental conditions. This conclusion is consistent with other electrospray studies showing that

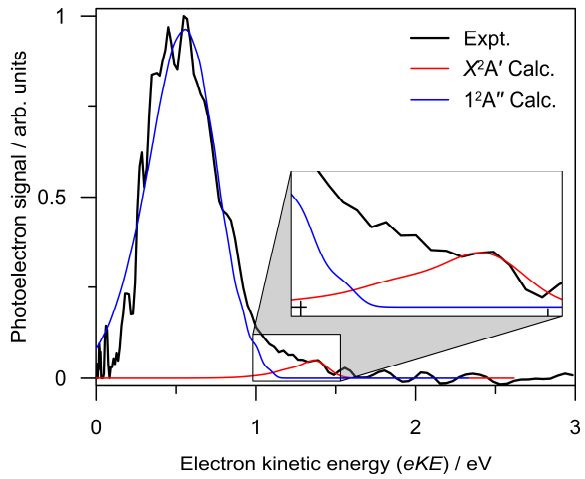

Fig. 3: 'Prompt detachment' spectrum at $h\nu$ = 4.13 eV (300 nm) – see text for further details. Also included are the Franck-Condon simulations for direct photodetachment to the X^2A' and $1^2A''$ neutral states. The maximum in calculated detachment cross-section for the $1^2A''$ TDDFT Franck-Condon spectrum has been translated in order to agree with the XMCQDPT2 excited state neutral energetics.

polarity-matched solvents and solutes tend to produce statistical/thermodynamic gas-phase products.[60,61] In addition, vibrationally-resolved photodetachment spectroscopy,[62,63] and mass spectrometry on the naphthyl anion,[64] as well as *ab initio* calculations on a range of PAH species,[65,66] indicate a very strong propensity to remove the most weakly bound proton during 'soft' anion formation.

Based on the above assignment of the deprotontation site, the prompt detachment spectrum can be assigned. Included in Fig. 3 are Franck-Condon simulations of the direct detachment spectrum to the X^2A' neutral state (red), and to the $1^2A''$ first excited neutral state (blue). The weak $1.0 \geq eKE \geq 1.5$ eV tail results from direct photodetachment forming the X^2A' neutral state, while the intense $0 \geq eKE \geq 1.0$ eV contribution corresponds to formation of the $1^2A''$ neutral state. The probable reason for the larger cross-section to produce the $1^2A''$ state relative to the X^2A' ground state is because the latter involves loss of an electron involved in Hückel aromaticity,[67] while the former involves loss of a carbon lone pair electron. Comparison between experiment and theory allows the VDE to the $1^2A''$ state to be determined at 3.5 ± 0.1 eV. Higher-lying neutral excited states become available at $h\nu > 4.2$ eV.

Calculated resonances, anionic bound state and neutral energetics, as well as relevant oscillator strengths are summarised in Fig. 4 assuming $C_{18}H_{11}^-$ deprotonated at site 1. Also included in Fig. 4 are the main CASSCF wavefunction configurations of each electronic state. Corresponding CASSCF natural orbitals are given in Fig. 5. The calculations identify four bound singlet excited states, two bound triplet states, and four singlet resonances within the maximum $h\nu$ in the current experiments (4.13 eV). Note that all energies are given as vertical excitation energies assuming the ground electronic anion state geometry. The CASSCF wavefunctions enable the classification of $4^1A''$ as a Feshbach resonance relative to the ground neutral state (X^2A'), while the higher-lying $2^1A'$, $3^1A'$, and $4^1A'$ resonances have shape character relative to the $1^2A''$ state of the neutral and Feshbach character with respect to the X^2A' neutral ground state.

As a comparison with electron attachment, Burrow and co-workers[22,68] reported measurements on closed-shell (not deprotonated) neutral tetracene, identifying at least six resonances up to 3 eV above-threshold. They present a correlation diagram that nicely summarises the rapid increase in the number of resonances and development of a band structure across the linear acene series from benzene to tetracene. The principal difference in electronic structure between neutral $C_{18}H_{12}$ and deprotonated $C_{18}H_{11}$ is the large increase in electron affinity for the latter, meaning that some low-lying anion resonances in tetracene become bound in deprotonated $C_{18}H_{11}^-$. Nevertheless, we expect a similar sequence of electron attachment dynamics between the two species, ultimately leading to long-lived anions.[30] We note a $h\nu$ = 3.49 eV (355 nm) PE spectrum of the tetracene radical anion has been reported by Mitsui *et al.*[51], although due to the use of a magnetic bottle spectrometer has been truncated at low-*eKE* where the thermionic feature is situated.

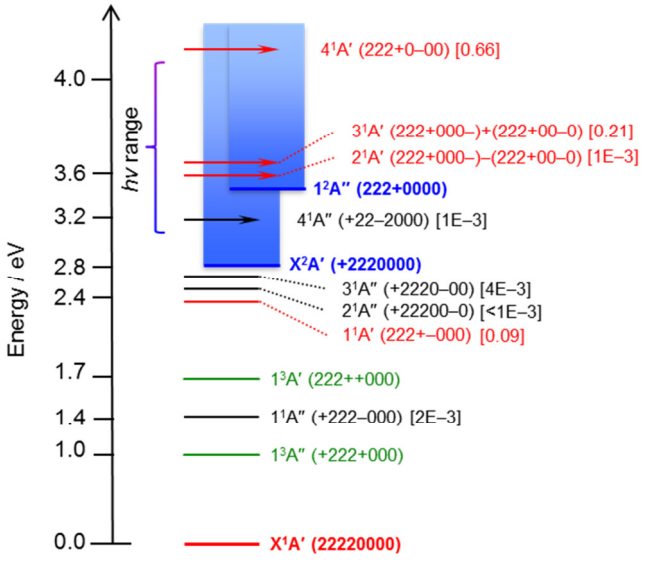

Fig. 4: Calculated resonances and excited states of $C_{18}H_{11}^-$ (deprotonated at site 1) at the multi-state XMCQDPT2/CASSCF(8,13)/6-31+G(d,p) level of theory. Also included are the main CASSCF configuration weights in parentheses (see Fig. 5 for illustrations of the corresponding orbitals), and oscillator strengths in square brackets. Key: black are singlet states of A″ symmetry; red are states of A′ symmetry; green are triplet states; blue are neutral electronic states; and arrows indicate the continuum with which the resonances correlate in a Koopmans picture.

Table 1 – Summary of electron detachment parameters, in units of eV, for each deprotonation site of tetracene (see Fig. 1). Calculated parameters at the ωB97XD//6-311++G(2df,2pd)+C*p* level of theory and (CCSD(T)/6-31+G(d,p) in parentheses).

Property	Site 1	Site 2	Site 3	Experiment
AEA	2.68 (2.52)	1.58	1.51	2.6 ± 0.2
VDE	2.76 (2.54)	1.97	1.88	2.8 ± 0.2

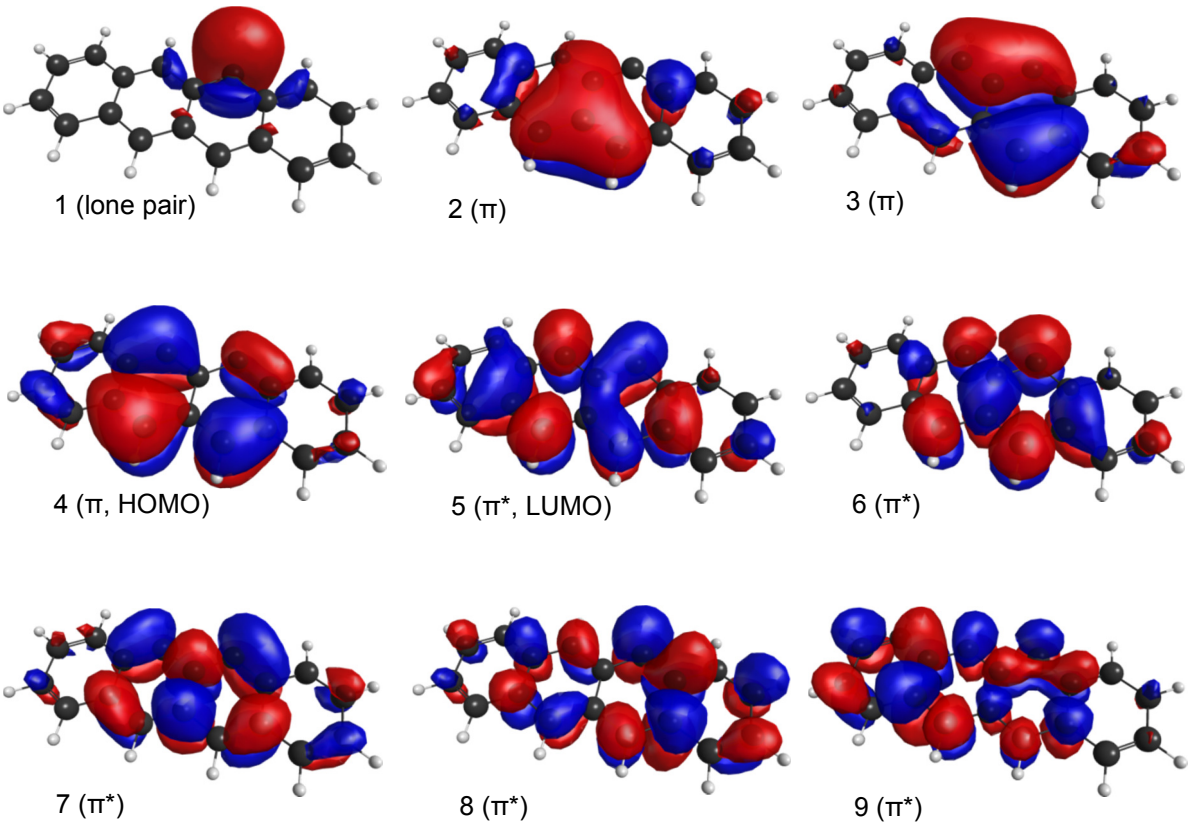

Fig. 5: Illustrations of the first nine natural orbitals in the CASSCF active space. Orbital 1 has A′ symmetry and all other orbitals have A″ symmetry. Other CASSCF orbitals in the active space (not shown) have negligible contribution to any state in Fig. 4.

Thermionic emission

The low-*eKE* Boltzmann-like PE feature, which is present in all PE spectra in Fig. 2, results from statistical electron emission from the ground electronic state of $C_{18}H_{11}^-$.[26,33-37] That is, excess internal energy statistically accumulates amongst certain modes leading to ejection of the most weakly bound electron. The properties, typical lifetimes (micro- to milliseconds), and mathematical description of thermionic emission have been well-reviewed in the aforementioned references. The observation of thermionic emission must be preceded by internal conversion of the photoexcited resonances. If the initial photoexcited (or intermediate) resonances were to spontaneously autodetach, only high-*eKE* features associated with the resonance binding energy would be observed in the PE spectrum. Instead, all PE spectra show that thermionic emission is the ultimate fate of most above-threshold photoexcitation. We stress that only a very small fraction of the true thermionic emission yield is collected in these spectra – *i.e.*, taking a thermionic emission lifetime of 10 ms implies that <0.01% of the thermionic electrons were collected.[30] The assumed lifetime of 10 ms, which was experimentally characterized for tetracene from electron attachment, is likely close to that for $C_{18}H_{11}^-$ since both have similar electronic structure and number of degrees of freedom. In fact, based the theory of thermionic emission,[33-37] the $C_{18}H_{11}^-$ thermionic emission lifetime may be expected to be longer than that for $C_{18}H_{12}^-$ due to a significantly increased AEA. Regardless, even in the unlikely case that the thermionic emission was a few orders of magnitude faster, the vast majority of the initial photoexcited resonance population would still internally convert to form the ground electronic state anion. The predominance of thermionic emission across all PE spectra is similar to that recently characterized for the radical anion of menadione, and suggests that $C_{18}H_{11}^-$ is resilient to direct photodetachment by broadband UV radiation.[26,69-74] Similarly, other results from our laboratory and from the Bordas group indicate that thermionic emission dominates the PE spectroscopy of C_{60}^- and other fullerene anions.[37,75] Such efficient ground state recovery dynamics is probably a generic feature of PAH anions, and would support their existence in favourable astrochemical environments.

The mechanism through which above-threshold population is funnelled to the ground electronic state is internal conversion *via* conical intersections that result from strong non-adiabatic electronic state couplings.[24-28] Complete internal conversion to the ground electronic state can be assisted by intermediate states that are close in energy, or by a ladder of intermediate states. In particular, bound electronic states of the anion have been shown to be important intermediates.[26] More generally, bound excited anion states are well-established to be important in the harvesting of solar energy in photovoltaic materials,[76] in biological and technological electron transfer systems,[26,40,77]

and in fluorescent proteins.[78-80] $C_{18}H_{11}^-$ has four bound singlet states (as well as two triplet states) providing a dense manifold for internal conversion (and intersystem crossing). Once the anion is in a bound electronic state, the excess internal energy becomes statistically redistributed amongst vibrational and rotational degrees of freedom and the system has more time to decay to the electronic ground state.

To directly probe whether such intermediate states are accessed in the present system requires the real-time measurement of internal conversion dynamics.[26] Unfortunately, such experiments were unsuccessful for $C_{18}H_{11}^-$ because: (i) there are multiple neutral states with overlapping Franck-Condon profiles that are available for probe photodetachment; (ii) by virtue of the high density of resonances the probe photon may induce further photoexcitation rather than photodetachment; and (iii) there are a number bound states through which relaxation dynamics can precede with overlapping Franck-Condon profiles. Hence, time-resolved PE spectroscopy of large PAH anions may be very difficult to interpret. Nevertheless, given the extremely efficient internal conversion to the ground state, bound intermediate states a very likely to be involved.

Formation of stable PAH anions

Although internal conversion is very efficient following electron capture, thermionic emission ultimately destroys the anion. Radiative cooling through infrared emission occurs on a timescale of seconds,[81-84] which will be a negligible channel compared with thermionic emission. Similarly, unimolecular dissociation rates in PAH anions are likely slower than thermionic emission because the bond dissociation energies are typically larger than the electron affinity. This situation may change for substituted PAHs.

Electronic state fluorescence processes are another mechanism that can contribute to radiative cooling without destroying the anion. In particular, certain molecules such as tetracene have been shown to undergo recurrent or Poincaré fluorescence.[85,86] In this process, a vibrationally-hot ground electronic state undergoes an inverse internal conversion to populate a bound electronic excited state, which then fluoresces. Bound excited states may also be populated in the forward internal conversion processes from the excited resonances and fluoresce. If radiative decay can compete with non-radiative decay of bound excited states, then a fluorescence photon could remove enough internal energy to close the thermionic emission channel and render the anion stable. While the present study provides no evidence for fluorescence, neutral tetracene has a recurrent fluorescence rate of ~50 ns.[87,88] Given that the rate of thermionic emission is likely several orders of magnitude slower, it is reasonable to conclude that recurrent fluorescence processes will allow production of some stable anions. Further, we note that the rate of recurrent fluorescence from tetracene is several orders of magnitude faster than that for smaller PAHs or species such as C_6^-.[89]

Since the rate of thermionic emission depends on the total internal energy, an increase in molecular size (total degrees of freedom) and/or AEA results in an increased thermionic emission lifetime. Concurrently, as size increases and the density of bound states increases, so does the likelihood of Poincaré fluorescence and the involvement of bound intermediate states in the non-adiabatic relaxation mechanism, which may also decay by fluorescence. In generalising to other PAH systems, increasing the number of rings in a linear acenes systematically increases the electron affinity,[90] while small non-linear PAHs have significantly reduced electron affinities.[91] Further, PAHs with nitrogen and oxygen atom substitutions may have similar bound electronic states, and are also candidates for astrochemical species.[4,7,92] Overall, such trends provide a basis for suggesting that larger PAH anions may be found in higher density and optically dark environments.

Role of non-adiabatic dynamics in astrochemistry

To date, six anions have been unequivocally identified to exist in the interstellar medium, C_4H^-, C_6H^-, C_8H^-, CN^-, C_3N^-, and C_5N^-.[12-18] These anions are all closed-shell with AEAs >3.5 eV, are highly conjugated, and have (valance-localized) π^*-resonances. The most commonly speculated mechanism for their formation is through capture of a very low energy electron (tens of meV) into a highly diffuse dipole-bound state by virtue of a very large capture cross-section.[19,20] However, we note that the neutral ground state of C_4H does not have a sufficient permanent dipole moment (>2.5 D) to support such a mechanism, nor do many other closed-shell and parent hydrogenated neutrals, e.g. C_nH_2 ($n = 2 - \infty$), and most PAH neutrals. Further, even if a neutral molecule captures an electron through a dipole-bound state, the total internal energy remains above the detachment threshold, so the system will be similarly subject to thermionic emission and other processes such as photoemission and fragmentation.

The process of electron attachment to resonances followed by internal conversion may provide an alternative or additional route to the formation of interstellar PAH anions. A number of recent theoretical studies, on systems that are known to exhibit long-lived anions in the gas phase, have supported this contention by highlighting that the above-threshold resonances of shape character have broad electron acceptance windows.[93-95] Experimentally, such a broad window to electron attachment dynamics has been observed across a range of PAH and PAH-like systems, [22,30,38] and has been implied in the present study by virtue of thermionic emission observed at all photoexcitation energies. The broad electron acceptance window arises from a combination of a high density of resonances (increases with increasing PAH size) each with a broad spectral width due to their inherent short lifetimes (e.g. a 25 fs lifetime corresponds to ~200 cm^{-1} width). When the probability of resonance electron capture is integrated over all available energies of the electrons, the total capture cross-section may become significant, particularly for PAHs that do not possess a sufficient dipole moment to support a dipole-bound state. Finally, we note that our results demonstrate that above-threshold photoexcitation can convert UV/visible radiation into low energy electrons (by thermionic emission).

Conclusions

In summary, we have presented photoelectron spectra combined with electronic structure calculations on a site-specific isomer of deprotonated tetracene anions, $C_{18}H_{11}^-$, which is a prototypical PAH. We have characterized that the combined yield of electrons from direct photodetachment and fast autodetachment in the 380 nm (3.26 eV) to 300 nm (4.13 eV) range is several orders of magnitude less than that for broadband photoexcitation to π*-resonances followed by thermionic emission on a millisecond timescale. By virtue of the same non-adiabatic dynamics, $C_{18}H_{11}^-$ is resilient to prompt photodestruction by UV radiation. Provided some radiative mechanisms of energy liberation are in competition with thermionic emission, the π*-resonance dynamics of $C_{18}H_{11}^-$ could facilitate formation of stable anions in astrochemical environments.

Due to the fact that similar π*-resonances occur in all highly conjugated molecules, such as C_nH, C_nH_2, C_nCN ($n = 2 - \infty$), PAHs, and general olefin chains, it is reasonable to suggest that the capture of electrons by a resonance may be a common process in some astrochemical environments – particularly for neutral molecules with a small or no permanent electric dipole moment. Further, the non-adiabatic processes discussed herein are a means through which electrons of a few eV or UV photons can be efficiently converted to free electrons of near zero kinetic energy.

Acknowledgements

Funding was provided by the European Research Council (Starting Grant 306536).

References

1. Neilson, A. H., Ed. *PAHs and Related Compounds;* Springer, 2010.
2. T. M. Figueira-Duarte and K. Müllen, *Chem. Rev.*, 2011, **111**, 7260.
3. X. Guo, M. Baumgarten and K. Müllen, *Prog. Poly. Sci.*, 2013, **38**, 1832.
4. A. G. G. M. Tielens, *Annu. Rev. Astron. Astrophys.*, 2008, **46**, 289.
5. S. Kwok and Y. Zhang, *Nature*, 2011, **479**, 80.
6. M. Larsson, W. D. Geppert and G. Nyman, *Rep. Prog. Phys.*, 2012, **75**, 066901.
7. A. G. G. M. Tielens, *Rev. Mod. Phys.*, 2013, **85**, 1021.
8. G. Israël, C. Szopa, F. Raulin, M. Cabane, H. B. Niemann, S. K. Atreya, S. J. Bauer, J.-F. Brun, E. Chassefière, P. Coll, E. Condé, D. Coscia, A. Hauchecorne, P. Millian, M.-J. Nguyen, T. Owen, W. Riedler, R. E. Samuelson, J.-M. Siguier, M. Steller, R. Sternberg and C. Vidal-Madjar, *Nature*, 2005, **438**, 796.
9. A. J. Coates, F. J. Crary, G. R. Lewis, D. T. Young, J. H. W. Jr. and E. C. S. Jr., *Geophys. Res. Lett.*, 2007, **34**, L22103.
10. C. Walsh, N. Harada, E. Herbst and T. J. Miller, *Astrophys. J.*, 2009, **700**, 752.
11. R. C. Fortenberry, *J. Phys. Chem. A*, 2015, doi: 10.1021/acs.jpca.5b05056.
12. M. C. McCarthy, C. A. Gottlieb, H. Gupta and P. Thaddeus, *Astrophys. J.*, 2006, **652**, L141.
13. J. Cernicharo, M. Guélin, M. Agúndez, K. Kawaguchi, M. C. McCarthy and P. Thaddeus, *Astrom. Astrophys.*, 2007, **467**, L37.
14. S. Brünken, H. Gupta, C. A. Gottlieb, M. C. McCarthy and P. Thaddeus, *Astrophys. J.*, 2007, **664**, L43.
15. A. J. Remijan, J. M. Hollis, F. J. Lovas, M. A. Cordiner, T. J. Miller, A. J. Markwick-Kemper and P. R. Jewell, *Astrophys. J*, 2007, **664**, L47.
16. P. Thaddeus, C. A. Gottlieb, H. Gupta, S. Brünken, M. C. McCarthy, M. Agúndez, M. Guélin and J. Cernicharo, *Astrophys. J.*, 2008, **667**, 1132.
17. J. Cernicharo, M. Guélin, M. Agúndez, M. C. McCarthy and P. Thaddeus, *Astrophys. J.*, 2008, **688**, L83.
18. M. Agúndez, J. Cernicharo, M. Guélin, C. Kahane, E. Roueff, J. Kłos, F. J. Aoiz, F. Lique, N. Marcelino, J. R. Goicoechea, M. González Garciá, C. A. Gottlieb, M. C. McCarthy and P. Thaddeus, *Astron. Astrophys.*, 2010, **517**, L2.
19. P. J. Sarre, *Mon. Not. R. Astron. Soc.*, 2000, **313**, L14.
20. K. D. Jordan and F. Wang, *Annu. Rev. Phys. Chem.*, 2003, **54**, 367.
21. H. S. Taylor, G. V. Nazaroff and A. Golebiewski, *J. Chem. Phys.*, 1966, **45**, 2872.
22. K. D. Jordan and P. D. Burrow, *Chem. Rev*, 1987, **87**, 557.
23. J. Simons, *J. Phys. Chem. A*, 2008, **112**, 6401.
24. M. Bixon and J. Jortner, *J. Chem. Phys.*, 1968, **48**, 715.
25. M. Baer. *Beyond Born-Oppenheimer: Electronic Nonadiabatic Coupling Terms and Conical Intersections;* Wiley, 2006.
26. J. N. Bull, C. W. West and J. R. R. Verlet, *Chem. Sci.*, 2015, **6**, 1578.
27. J. N. Bull, C. W. West and J. R. R. Verlet, *Phys. Chem. Chem. Phys.*, 2015, **17**, 16125.
28. D. A. Horke, Q. Li, L. Blancafort and J. R. R. Verlet, *Nat. Chem.*, 2013, **5**, 711.
29. M. Allan, *J. Elect. Spectro. Rel. Phenom.*, 1989, **48**, 219.
30. R. V. Khatymov, R. F. Tukatrov and M. V. Muftakhov, *JTEP Lett.*, 2011, **93**, 437.
31. P. L. Houston. *Chemical Kinetics and Reaction Dynamics;* Dover Publications, 2006.
32. N. E. Henriksen and F. Y. Hansen. *Theories of Molecular Reaction Dynamics: The Microscopic Foundation of Chemical Kinetics;* Oxford University Press, 2012.
33. E. E. B. Campbell, G. Ulmer and I. V. Hertel, *Phys. Rev. Lett.*, 1991, **67**, 1986.
34. A. Amrein, R. Simpson and P. Hackett, *J. Chem. Phys.*, 1991, **95**, 1781.
35. B. Climen, F. Pagliarulo, A. Ollagnier, B. Baguenard, B. Concina, M. A. Lebeault, F. Lepiné and C. Bordas, *Eur. Phys. J. D*, 2007, **43**, 85.
36. J. C. Pinaré, B. Baguenard, C. Bordas and M. Broyer, *Phys. Rev. Lett.*, 1998, **81**, 2225.
37. B. Concina, F. Lépine and C. Bordas, *Phys. Rev. A*, 2014, **90**, 033415.
38. N. L. Asfandiarov, S. A. Pshenichnyuk, A. S. Vorob'ev, E. P. Nafikova, Y. N. Elkin, D. N. Pelageev, E. A. Koltsova and A. Modelli, *Rapid Commun. Mass Spectrom.*, 2014, **28**, 1580.
39. N. J. Demarais, Z. Yang, O. Martinex Jr., N. Wehres, T. P. Snow and V. M. Bierbaum, *Astrophys. J.*, 2012, **746**, 32.
40. D. A. Horke, G. M. Roberts and J. R. R. Verlet, *J. Phys. Chem. A*, 2011, **115**, 8369.
41. D. A. Horke, G. M. Roberts, J. Lecointre and J. R. R. Verlet, *Rev. Sci. Instrum.*, 2012, **83**, 062101.
42. A. T. J. B. Eppink and D. H. Parker, *Rev. Sci. Instrum.*, 1997, **68**, 3477.
43. G. M. Roberts, J. L. Nixon, J. Lecointre, E. Wrede and J. R. R. Verlet, *Rev. Sci. Instrum.*, 2009, **80**, 053104.
44. R. N. Zare, *Mol. Photochem.*, 1972, **4**, 1.
45. M. J. Frisch, G. W. Trucks, H. B. Schlegel, G. E. Scuseria, M. A. Robb, J. R. Cheeseman, G. Scalmani, V. Barone, B. Mennucci, G. A. Petersson, H. Nakatsuji, M. Caricato, X. Li, H. P. Hratchian, A. F. Izmaylov, J. Bloino, G. Zheng, J. L. Sonnenberg, M. Hada, M. Ehara, K. Toyota, R. Fukuda, J. Hasegawa, M. Ishida, T. Nakajima, Y. Honda, O. Kitao, H. Nakai, T. Vreven, Jr., J. A. Montgomery, J. E. Peralta, F. Ogliaro, M. Bearpark, J. J. Heyd, E. Brothers, K. N. Kudin, V. N. Staroverov, R. Kobayashi, J. Normand, K. Raghavachari, A. Rendell, J. C. Burant, S. S. Iyengar, J. Tomasi, M. Cossi, N. Rega, N. J. Millam, M. Klene, J. E. Knox, J. B. Cross, V. Bakken, C. Adamo, J. Jaramillo, R. Gomperts, R. E. Stratmann, O. Yazyev, A. J. Austin, R. Cammi, C. Pomelli, J. W.

Ochterski, R. L. Martin, K. Morokuma, V. G. Zakrzewski, G. A. Voth, P. Salvador, J. J. Dannenberg, S. Dapprich, A. D. Daniels, Ö. Farkas, J. B. Foresman, J. V. Ortiz, J. Cioslowski and D. J. Fox. *Gaussian, Inc.;* Tech. rep.; Wallingford CT, 2009.

46. M. W. Schmidt, K. K. Baldridge, J. A. Boatz, S. T. Elbert, M. S. Gordon, J. H. Jensen, S. Koseki, N. Matsunaga, K. A. Nguyen, S. Su, T. L. Windus, M. Dupuis and J. A. Montgomery Jr., *J. Comput. Chem.*, 1993, **14**, 1347.
47. J.-D. Chai and M. Head-Gordon, *Phys. Chem. Chem. Phys.*, 2008, **10**, 6615.
48. R. Krishnan, J. S. Binkley, R. Seeger and J. A. Pople, *J. Chem. Phys.*, 1980, **72**, 650.
49. A. J. . M.-S. P. . Y. W. Cohen, *Science*, 2008, **321**, 792.
50. F. Jensen, *J. Chem. Theory Comput.*, 2010, **6**, 2726.
51. M. Mitsui, N. Ando and A. Nakajima, *J. Phys. Chem. A*, 2007, **111**, 9644.
52. V. Barone, J. Bloino, M. Biczysko and F. Santoro, *J. Chem. Theory and Comput.*, 2009, **5**, 540.
53. J. A. Pople, M. Head-Gordon and K. Raghavachari, *J. Chem. Phys.*, 1987, **87**, 5968.
54. R. E. Stratmann, G. E. Scuseria and M. J. Frisch, *J. Chem. Phys.*, 1998, **109**, 8218.
55. J. S.-Y. Chao, M. F. Falcetta and K. D. Jordan, *J. Chem. Phys.*, 1990, **93**, 1125.
56. A. A. Granovsky, *J. Chem. Phys.*, 2011, **134**, 214113.
57. C. W. West, J. N. Bull, E. Antonkov and J. R. R. Verlet, *J. Phys. Chem. A*, 2014, **118**, 11346.
58. E. P. Wigner, *Phys. Rev.*, 1948, **73**, 1002.
59. K. J. Reed, A. H. Zimmerman, H. C. Andersen and J. I. Brauman, *J. Chem. Phys.*, 1976, **64**, 1368.
60. D. Schröder, M. Buděšínský and J. Roithová, *J. Am. Chem. Soc.*, 2012, **134**, 15897.
61. A. Kruve, K. Kaupmees, J. Liigand and I. Leito, *Anal. Chem.*, 2014, **86**, 4822.
62. M. L. Weichman, J. B. Kim, J. A. DeVine, D. S. Levine and D. M. Neumark, *J. Am. Chem. Soc.*, 2015, **137**, 1420.
63. K. M. Ervin, T. M. Ramond, G. E. Davico, R. L. Schwartz, S. M. Casey and W. C. Lineberger, *J. Phys. Chem. A*, 2001, **105**, 10822.
64. D. R. Reed and S. R. Kass, *J. Mass Spectrom.*, 2000, **35**, 534.
65. V. Van Speybroeck, G. B. Marin and M. Waroquier, *Chem. Phys. Chem.*, 2006, **7**, 2205.
66. K. Hemelsoet, V. Van Speybroeck and M. Waroquier, *J. Phys. Chem. A*, 2008, **112**, 13566.
67. E. Hückel, *Z. Physik*, 1931, **70**, 204.
68. P. D. Burrow, J. A. Michejda and K. D. Jordan, *J. Chem. Phys.*, 1987, **86**, 9.
69. G. Mulas, A. Zonca, S. Casu and C. Cecchi-Pestellini, *Astrophys. J. Supp. Ser.*, 2013, **207**, 7.
70. G. C. Clayton, K. D. Gordon, F. Salama, L. J. Allamandola, Peter G. Martin, T. P. Snow, D. C. B. Whittet, A. N. Witt and M. J. Wolff, *Astrophys. J.*, 2003, **592**, 947.
71. A. Ricca, C. W. B. Jr., C. Boersma, A. G. G. M. Tielens and L. J. Allamandola, *Astrophys. J.*, 2012, **754**, 75.
72. G. Malloci, G. Mulas and C. Joblin, *Astron. Astrophys.*, 2004, **426**, 105.
73. C. Cecchi-Pestellini, G. Malloci, G. Mulas, C. Joblin and D. A. Williams, *Astron. Astrophys.*, 2008, **486**, L25.
74. M. Steglich, Y. Carpentier, C. Jäger, F. Huisken, H.-J. Räder and Th. Henning, *Astron. Astrophys.*, 2012, **540**, A110.
75. Antonkov, E., C. W. West, J. N. Bull and J. R. R. Verlet, *Unpublished*.
76. T. Liu and A. Troisi, *Adv. Mater.*, 2013, **25**, 1038.
77. S. B. Nielsen and J. A. Wyer. *Photophysics of Ionic Biochromophores;* Springer-Verlag, 2013.
78. C. W. West, A. S. Hudson, S. L. Cobb and J. R. R. Verlet, *J. Chem. Phys.*, 2013, **139**, 071104.
79. C. W. West, J. N. Bull, A. S. Hudson, S. L. Cobb and J. R. R. Verlet, *J. Phys. Chem. B.*, 2015, **119**, 3982.
80. A. V. Bochenkova, B. Klærke, D. B. Rahbek, J. Rajput, Y. Toker and L. H. Andersen, *Angew. Chem. Int. Ed.*, 2014, **53**, 9797.
81. S. Martin, J. Bernard, R. Bredy, B. Concina, C. Joblin, M. Ji, C. Ortega and L. Chen, *Phys. Rev. Lett.*, 2013, **110**, 063003.
82. E. L. O. Bakes, A. G. G. M. Tielens and C. W. B. Jr., *Astrophys. J.*, 2001, **556**, 501.
83. B. T. Draine and A. Li, *Astrophys. J.*, 2001, **551**, 807.
84. A. Li and B. T. Draine, *Astrophys. J.*, 2001, **554**, 778.
85. A. Léger, P. Boissel and L. d'Hendecourt, *Phys. Rev. Lett.*, 1988, **60**, 921.
86. A. Nitzan and J. Jortner, *J. Chem. Phys.*, 1979, **71**, 3524.
87. A. Amirav, U. Evan and J. Jortner, *J. Chem. Phys.*, 1981, **75**, 3770.
88. M. Baba, M. Saitoh, Y. Kowaka, K. Taguma, K. Yoshida, Y. Semba, S. Kasahara, T. Yamanaka, Y. Oshsima, Y.-C. Hsu and S. H. Lin, *J. Chem. Phys.*, 2009, **131**, 224318.
89. V. Chandrasekaran, B. Kafle, A. Prabhakaran, O. Heber, M. Rappaport, H. Rubinstein, D. Schwalm, Y. Toker and D. Zajfman, *J. Phys. Chem. Lett.*, 2014, **5**, 4078.
90. B. Hajgató, M. S. Deleuze, D. J. Tozer and F. De Proft, *J. Chem. Phys.*, 2008, **129**, 084308.
91. A. Modelli, L. Mussoni and D. Fabbri, *J. Phys. Chem. A*, 2006, **110**, 6482.
92. M. L. Theis, A. Candian, A. G. G. M. Tielens, T. J. Lee and R. C. Fortenberry, *Phys. Chem. Chem. Phys.*, 2015, **17**, 14761.
93. A. Garcia-Sanz, F. Carelli, F. Sebastianelli, F. A. Gianturco and G. Garcia, *New J. Phys.*, 2013, **15**, 013018.
94. F. Carelli, F. A. Gianturco, M. Satta and F. Sebastianelli, *Int. J. Mass Spectrom.*, 2014, **365-366**, 377.
95. M. L. Senet and M. Hochlaf, *Astrophys. J.*, 2013, **768**, 59.

